

C_nN^+ - He Collisions – Fundamental aspects and application to astrochemistry.



Thejus Mahajan¹, Karine Béroff¹ and AGAT Collaboration.^{1,2,3,4}

¹Institut des Sciences Moléculaires d'Orsay (ISMO), CNRS and Université Paris-Sud, 91405 Orsay, France.

²IRAP - UMR 5277 / Université de Toulouse [UPS-OMP] / CNRS.

³Institut de Physique Nucléaire Orsay (IPNO), CNRS and Université Paris-Sud, 91406 Orsay, France.

⁴Service de Chimie Quantique et Photophysique (SQP), Université Libre de Bruxelles, Brussels, Belgium.



In this work, we try to understand the process of excitation and fragmentation of C_nN^+ molecules in high velocity collisions with atoms. Experiments are conducted at the Tandem accelerator, Orsay. The motivation being the presence of such species in astrophysical environments, for instance the atmosphere of Titan. The collision is divided into two phases, excitation of the molecule in the first phase $\{10^{-16} \text{ s}\}$ then relaxation by fragmentation. The excitation phase will be modelled theoretically in collaboration with theoreticians in Madrid and Bordeaux. The data of fragmentation are relevant in the astrochemical domain and will be added to the recent international kinetic database KIDA where researchers all over the world will use the data.

Experimental set-up and methods

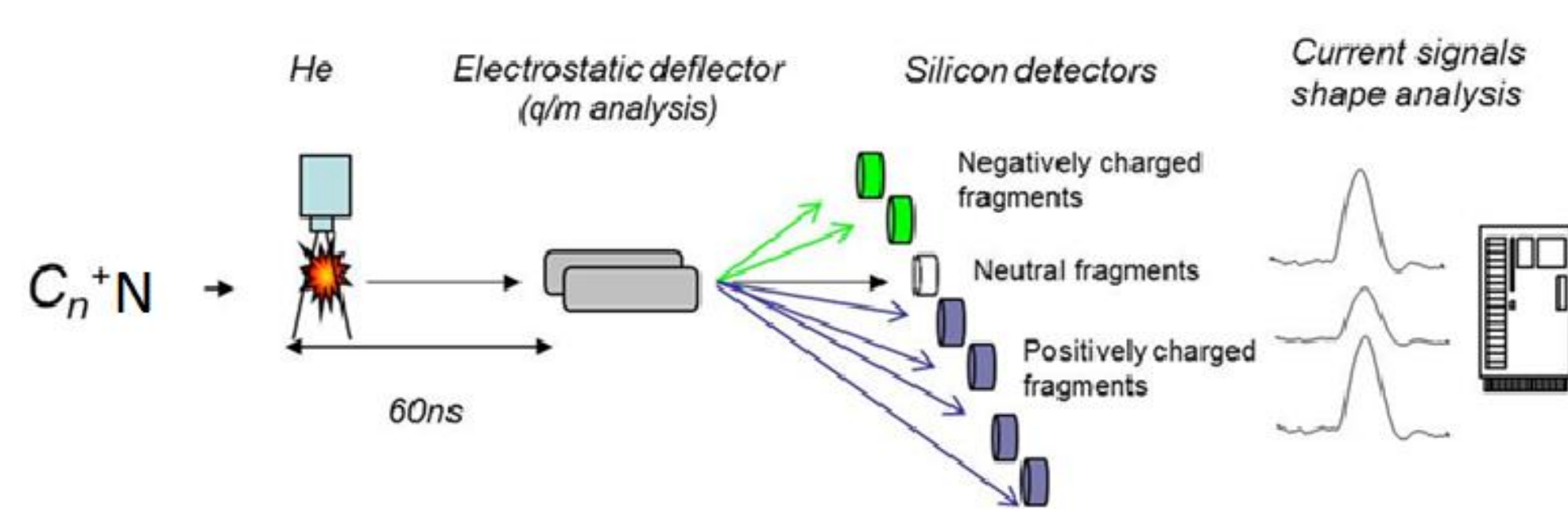


Fig 1. AGAT setup.

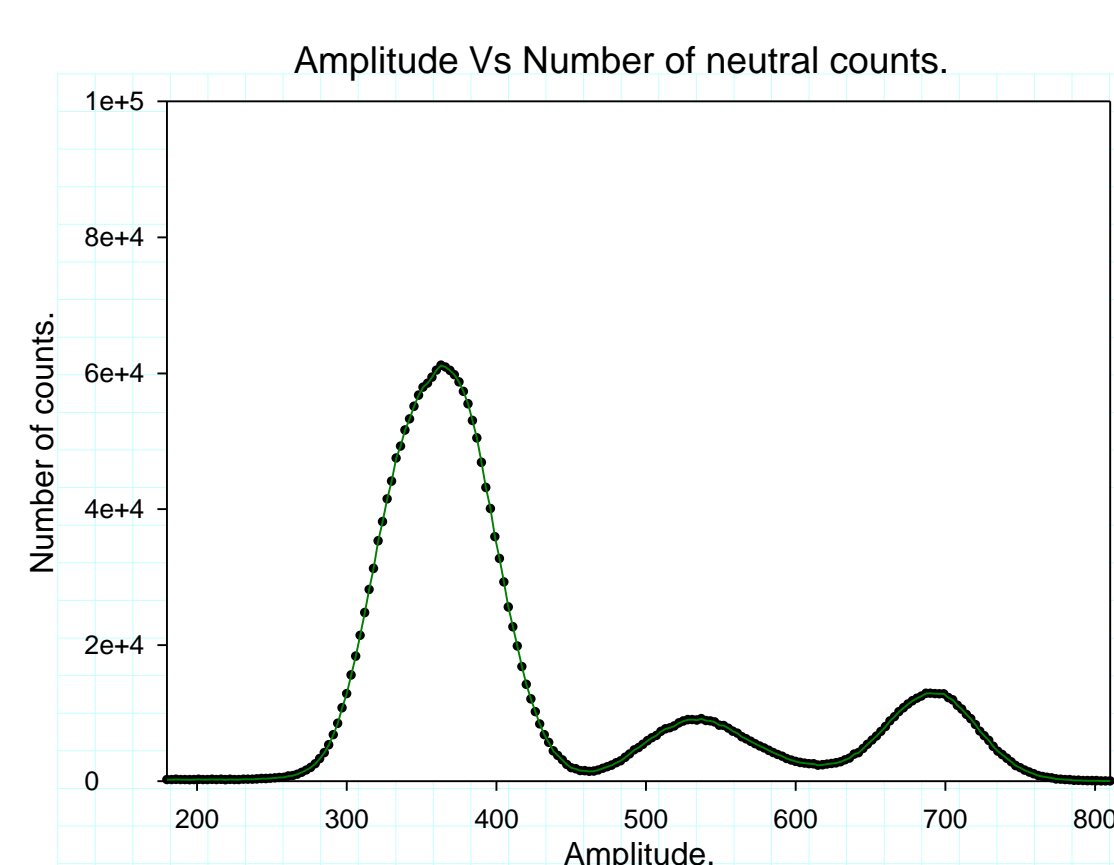


Fig 2. 1d - Amplitude vs Number of counts.

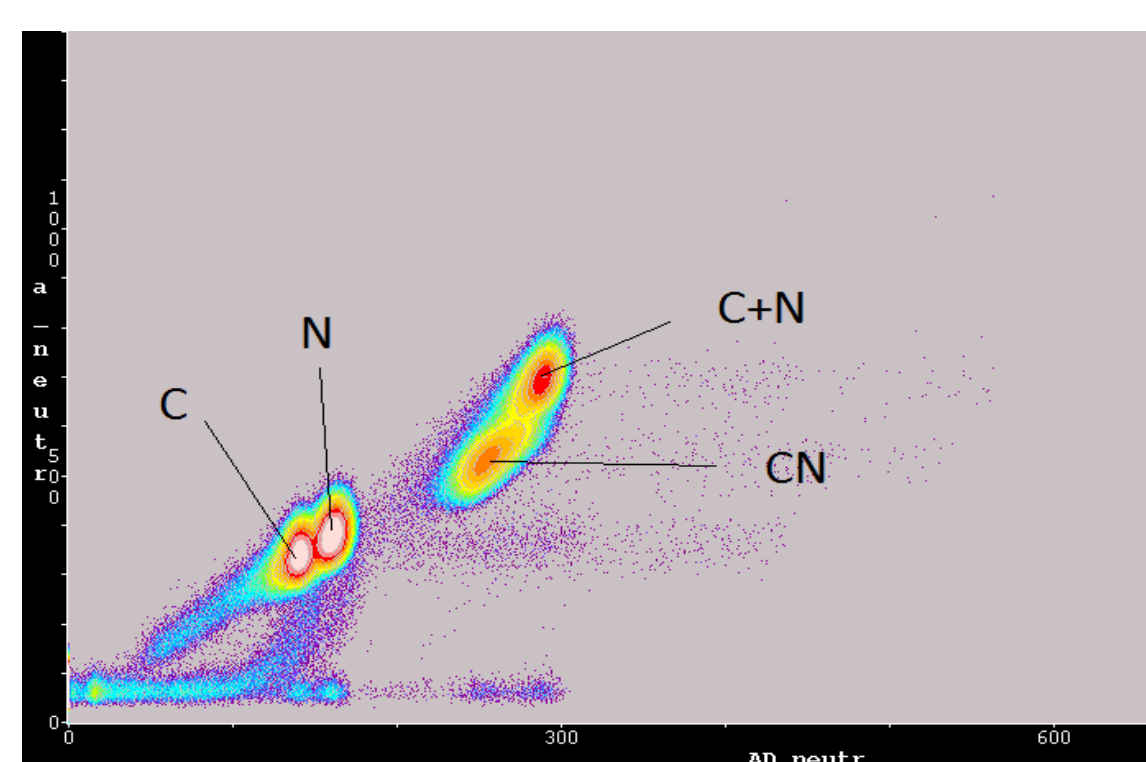


Fig 3. Two dimensional representation.

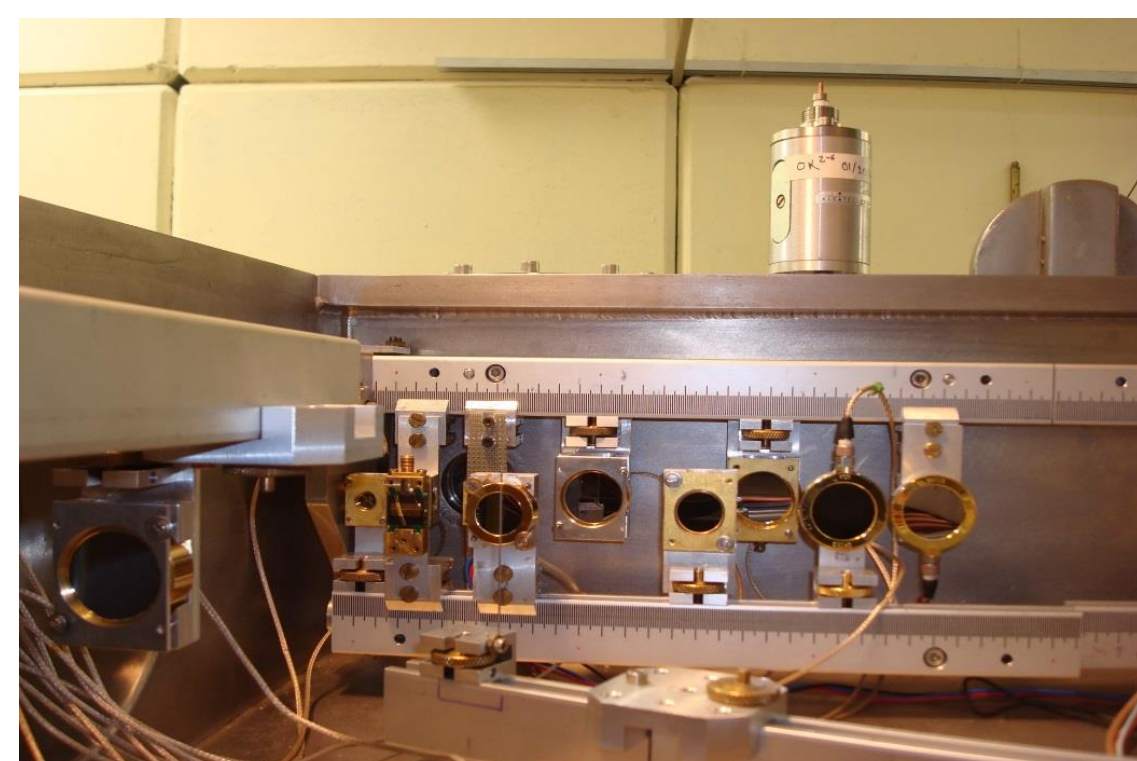


Fig 4. Silicon detectors

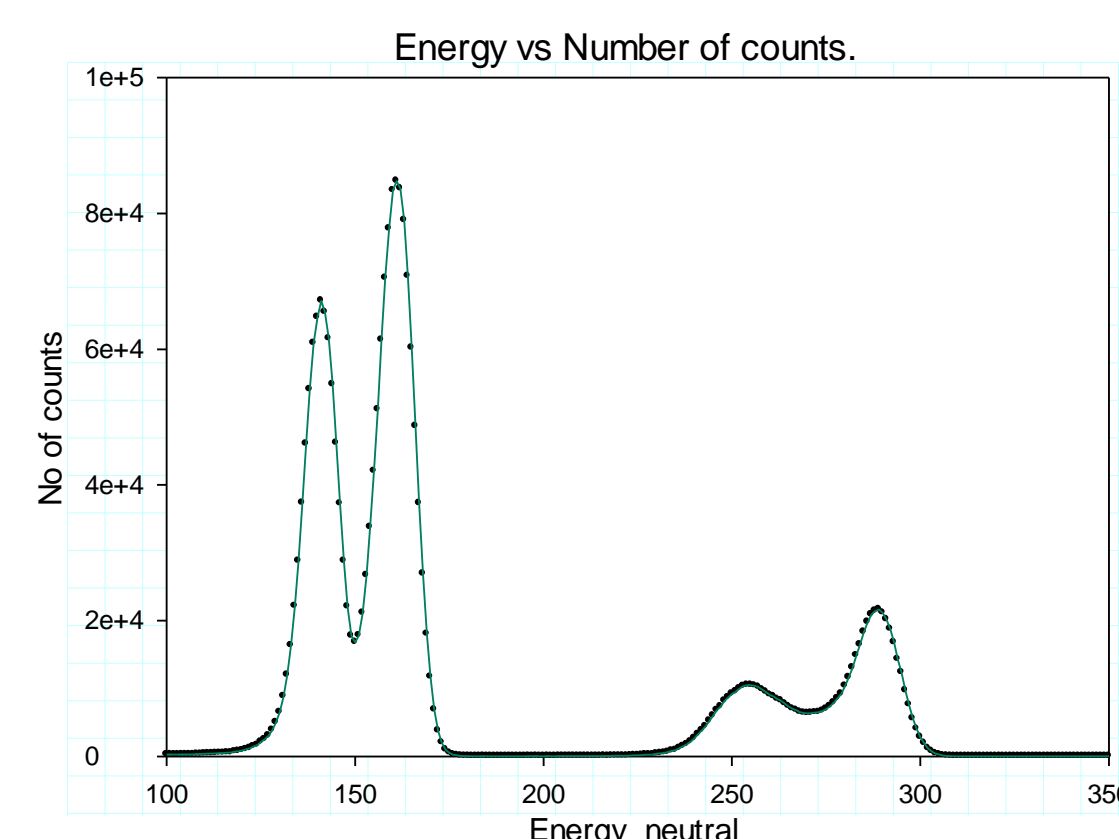


Fig 5. 1d - Energy vs Number of counts.

The analysis of the data from the silicon detectors Fig. 4 is done using a software DP2 [1] which is a 2D visualization and analysis software for multi-dimensional data. We design grids around patches Fig. 3 of interest. The one dimensional plots featuring amplitude and integral of the current signals are easily treated in 2d DP2 representation.

Absolute cross sections

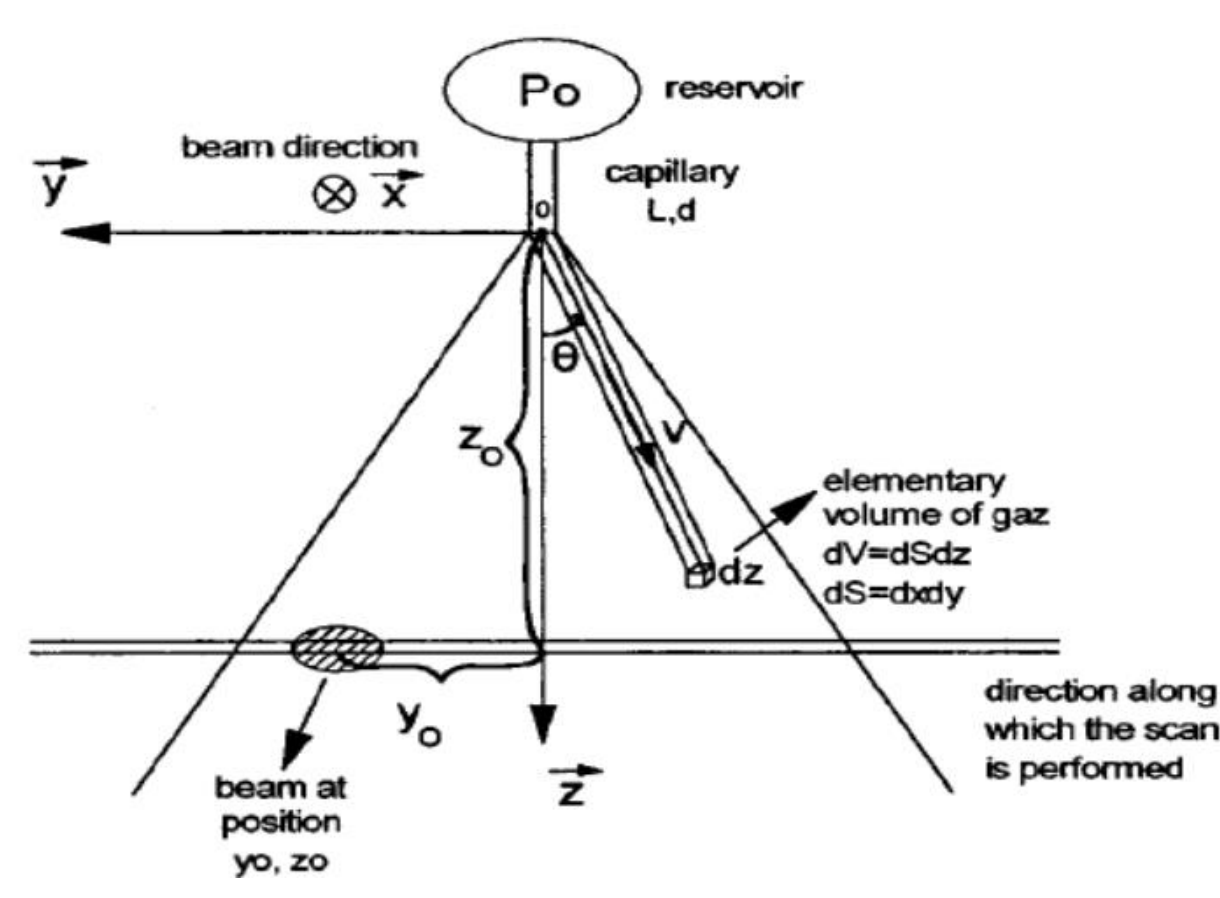


Fig 6. Schematic illustration of beam and jet relative positions [2].

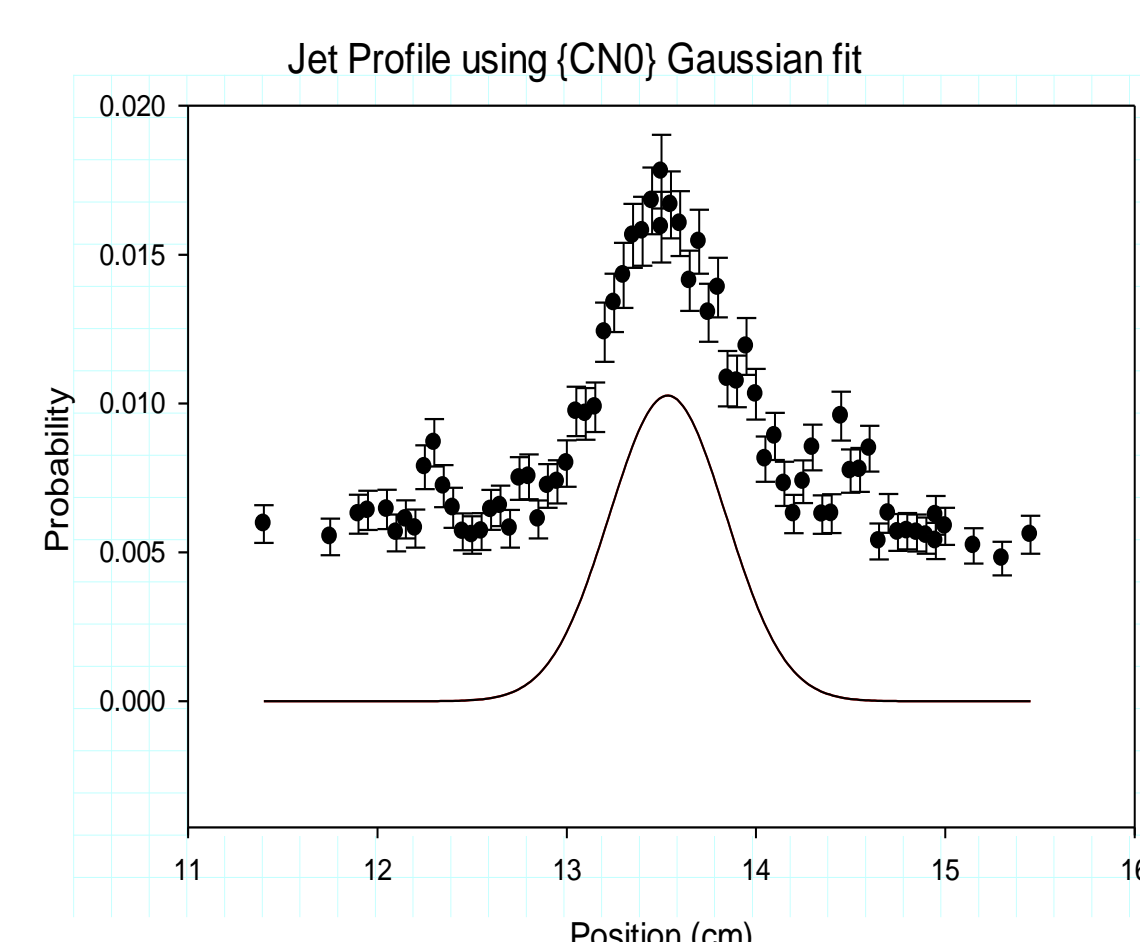


Fig 7. Measured jet profile

The cross section σ of an inelastic process is calculated by the following. For single collision the equations used [2] are

$$\sigma = \frac{\text{prob}(y_0, z_0)}{B_{\text{jet}}(y_0, z_0)} \quad (1) \quad \int \frac{\text{prob}(y_0, z_0)}{\text{prob}(y_0, z_0)} dy_0 = \frac{B_{\text{jet}}(y_0, z_0)}{\int B_{\text{jet}}(y_0, z_0) dy_0} \quad (2) \quad \int B_{\text{jet}}(y_0, z_0) dy_0 = \frac{dN}{dt} \frac{1}{\langle v_z \rangle} \quad (3)$$

The jet is scanned laterally in Fig. 6 along y , the probability of collision is measured at each point and $\text{prob}(y, z_0)$ at fixed z_0 is experimentally deduced. It can be shown that the denominator in Eq. (2) is related to the total flow rate of jet $\frac{dN}{dt}$ which is measured and mean velocity of the molecules in the jet $\langle v_z \rangle$ along z .

Cross section for anionic fragment production

There is a competition between single and double collisions. The single collision condition is

$$P = \sigma B_{\text{jet}} \quad (4)$$

But anionic production probabilities are found to be quadratic with B_{jet} . This leads to the conclusion that there is indeed not one but two collisions for their formations. In case of anionic production, probability of formation is taken as

$$P = \sigma_1 B_{\text{jet}} + \frac{\sigma_2 \sigma_3 B_{\text{jet}}^2}{2} \quad (5)$$

which is a polynomial equation of second order with respect to B_{jet} . The experimental data agrees with this prediction given in fig. 8. On dividing (4) with a probability of species following a single collision condition P_{norm} , we get the following

$$\frac{P}{P_{\text{norm}}} = \frac{\sigma_1}{\sigma_{\text{norm}}} + \frac{\sigma_2 \sigma_3}{2\sigma_{\text{norm}}} B_{\text{jet}} \quad (6)$$

which is a 1st order polynomial equation with intercept in Fig. 9 gives $\frac{\sigma_1}{\sigma_{\text{norm}}}$ and the slope gives, $\frac{\sigma_2 \sigma_3}{2\sigma_{\text{norm}}}$.

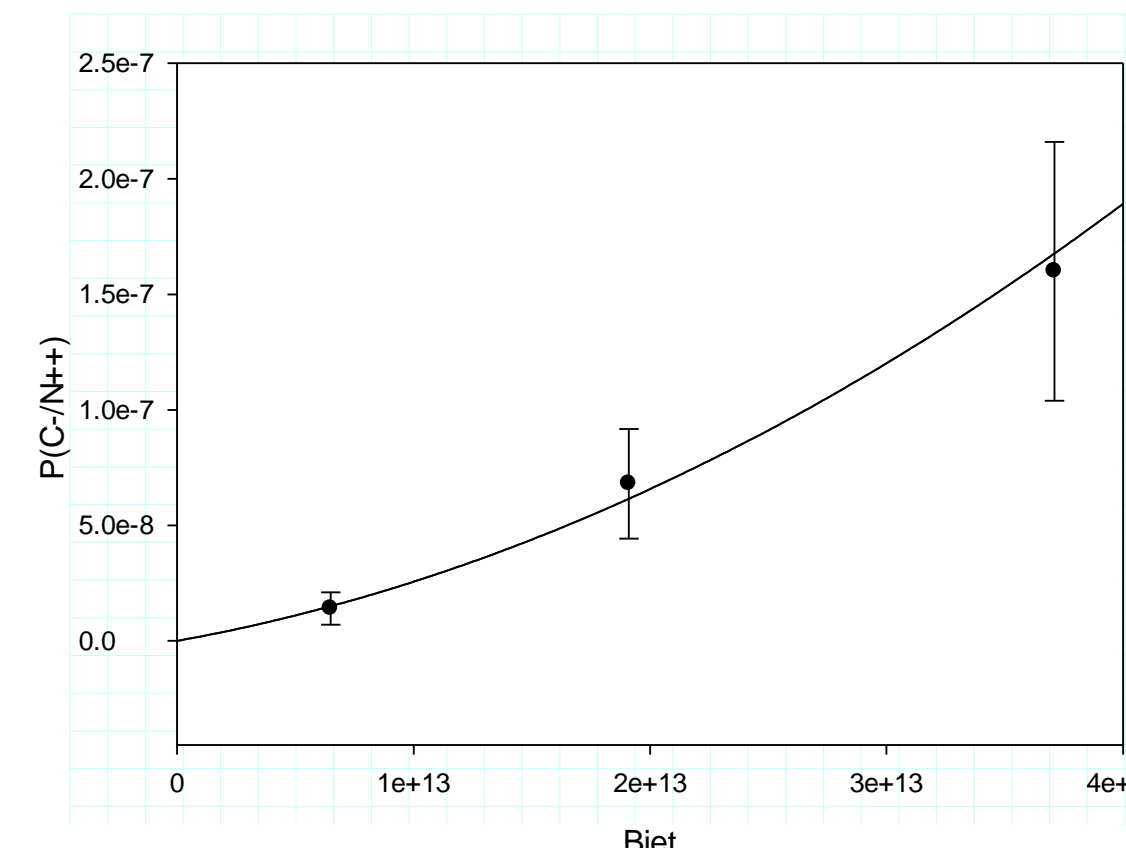


Fig 8. Evolution of P(C-/N++) with target thickness B_{jet}

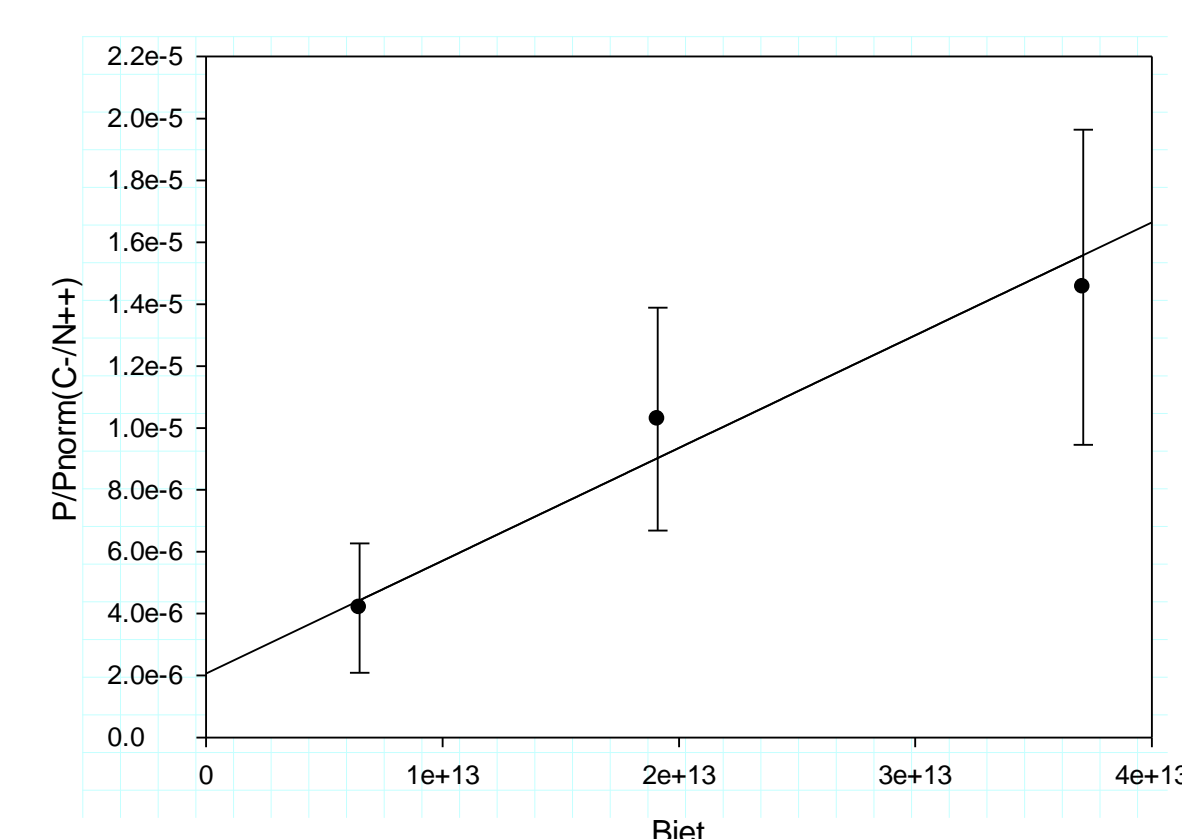


Fig 9. Evolution of P(Pnorm(C-/N++)) with target thickness B_{jet}

CN+ analysis results

Process (σ_i)	Cross section CN^+ (relative error in %) (cm^2)
σ_{DC} $CN^+ \rightarrow CN^-$	$3.9 \cdot 10^{-20}$ (21%)
σ_{SC} $CN^+ \rightarrow CN$	$4.15 \cdot 10^{-17}$ (17%)
σ_{ED} $CN^+ \rightarrow CN^+$	$9.44 \cdot 10^{-17}$ (18%)
σ_{SI} $CN^+ \rightarrow CN^{++}$	$2.29 \cdot 10^{-16}$ (19%)
σ_{DI} $CN^+ \rightarrow CN^{+++}$	$5.44 \cdot 10^{-17}$ (18%)
σ_{TI} $CN^+ \rightarrow CN^{++++}$	$8.28 \cdot 10^{-18}$ (18%)

Table 1. Measured cross sections of various processes (preliminary results).

Process of diatomic (AB^+) I.	Relaxation channels	BR 2.2 a.u. (relative error in %)	BR 3.6 a.u. (CN^+) [3]
BR(DC) $CN^+ \rightarrow \{CN^-\}$	C/N	0.02(201%)	
	CN^-	0.98(29%)	
BR(SC) $CN^+ \rightarrow \{CN\}$	C/N^+	0.001(27%)	
	C+N	0.55(1%)	0.5(1%)
	CN	0.45(1%)	0.5(1%)
BR(ED) $CN^+ \rightarrow \{CN^+\}$ *	C/N^{++}	0.00001(29%)	
	C^+/N	0.55(5%)	0.53(6%)
	CN^+	0.45(5%)	0.47(6%)
BR(SI) $CN^+ \rightarrow \{CN^{++}\}$	C^+/N^+	0.92(1%)	0.94(4%)
	C^{++}/N	0.052(1%)	0.04(50%)
	C/N^{++}	0.024(10%)	0.02(100%)
BR(DI) $CN^+ \rightarrow \{CN^{+++}\}$	C^{++}/N^+	0.58(8%)	0.61(5%)
	N^{++}/C^+	0.40(10%)	0.39(5%)
	N^{++}/C	$1.3 \cdot 10^{-3}$ (15%)	$1 \cdot 10^{-3}$ (100%)
	C^{+++}/N	$4.0 \cdot 10^{-3}$ (15%)	$4 \cdot 10^{-3}$ (25%)
BR(TI) $CN^+ \rightarrow \{CN^{++++}\}$	C^{+++}/N^+	0.1(3%)	0.15(6%)
	C^{++}/N^{++}	0.86(1%)	0.80(5%)
	N^{+++}/C^+	0.04(3%)	0.05(20%)

Table 2. Measured branching ratios and comparison with velocities 2.2 a.u and 3.6 a.u (preliminary results).

Future.

- Completing the analysis for other C_nN^+ .
- Another experiment in autumn 2016 with CCD (Charge Coupled Device) camera.
- Modelling of the collisions CTMC (Classical Trajectory Monte Carlo) simulation with Clara Illescas in Madrid.

References

- [1] L. Tassan-Got, personal communication, October 2015.
- [2] K. Wöhrer *et al.*, Rev. Sci. Instrum., **71**, 5 (2000).
- [3] A. Jallat (2015) PhD thesis.